Diabetes, Metabolic Syndrome and Obesity

Dovepress
Taylor & Francis Group

Open Access Full Text Article

ORIGINAL RESEARCH

The Shengmai San Exerts Therapeutic Effects on Type 2 Diabetes by Modulating the PI3K/AKT/GSK3B Signaling Pathway

Hongchao Shang, Tianyu Wang, Daoran Pang, Yue Qi, Lu Liu, Yifei Wang, Yan Gao

Institute of Pharmacy, Shandong University of Traditional Chinese Medicine, Jinan, 250355, People's Republic of China

Correspondence: Yan Gao, Institute of Pharmacy, Shandong University of Traditional Chinese Medicine, Jinan, 250355, People's Republic of China, Tel +18615212592, Email gaoyaningyes@163.com

Context: Shengmai San (SMS) is a traditional Classic Recipes made with Panax ginseng, Ophiopogon, and Schisandra. The precise mechanism of action of SMS remains unclear, despite its noteworthy therapeutic advantages for type 2 diabetes mellitus (T2DM).

Objective: The objective of this study was to confirm the mechanism of SMS in the treatment of T2DM.

Materials and Methods: UPLC-MS/MS was employed to identify the active components in SMS. Using network pharmacology, the intervention pathways of SMS in T2DM rats were investigated. A high-sugar, high-fat diet and intrabitoneal injection of streptozotocin were used to create a T2DM rat model. The serum parameters of each group were assessed following the completion of the experiment. The mRNA and protein expression levels of genes related to the PI3K/AKT/GSK3B pathway were analyzed using qRT-PCR and Western blot.

Results: There were 39 components found in SMS San by UPLC-Q-Orbitrap/MS. Network pharmacology and molecular docking study indicate that the PI3K/AKT/GSK3B pathway may be a part of SMS's therapeutic mechanism for the treatment of T2DM. Rats' serum levels of TC, TG, LDL-C, MDA, TNF-α, and IL-6 dramatically dropped after taking SMS, whereas SOD and HDL-C levels rose. The improvement of these parameters may be related to SMS activation of downstream target proteins, PI3K, and AKT.

Conclusion: SMS can help cure T2DM mellitus by regulating the PI3K/AKT/GSK3B pathway, improving islet tissue injury, reducing oxidative stress, and easing lipid metabolism issues. This study not only revealed the unique therapeutic mechanism of SMS by regulating the PI3K/AKT/GSK3β signaling pathway, but also provided new theoretical support for multi-target and personalized treatment of diabetes. Its novelty lies in the first exploration of the mechanism of action of traditional Chinese medicine prescriptions through the lens of modern molecular biology, emphasizing the potential of natural medicines in diabetes treatment.

Keywords: Shengmai San, network pharmacology, UPLC-MS/MS, type 2 diabetes mellitus, PI3K/AKT/GSK3B pathway

Introduction

In recent years, the incidence of diabetes has steadily increased. Epidemiological studies estimate that the global number of diabetic patients will rise from 371 million in 2000 to 589 million by 2025, with a further increase to 643 million by 2030.[1] Type 1 diabetes mellitus (T1DM), Type 2 diabetic mellitus (T2DM), gestational diabetes mellitus, and other forms are the four categories of diabetes. T2DM accounts for a noteworthy 90% of all occurrences of diabetes.[2] Cardiovascular disease is the leading cause of death in individuals with diabetes. Diabetes not only elevates the risk of cardiovascular damage but also contributes to subclinical blood sugar increases, which raise A1C levels even in individuals who do not meet the diagnostic criteria for diabetes. In individuals without diabetes, it also leads to subclinical cardiovascular dysfunction and an increased risk of developing overt cardiovascular disease. T2DM is a chronic metabolic disorder characterized by reduced insulin sensitivity, impaired glucose and lipid metabolism, or related metabolic imbalances.[3] Its pathogenesis may be linked to lipid metabolism disorders, where oxidative stress leads to islet tissue damage, decreased insulin secretion, reduced glucose uptake, diminished glycogen synthesis, increased glycogen breakdown, and elevated blood glucose levels. Current treatments for diabetes primarily involve oral hypoglycemic agents or insulin injections.[4]

Received: 22 November 2024
Accepted: 11 March 2025
Published: 2 April 2025

Graphical Abstract

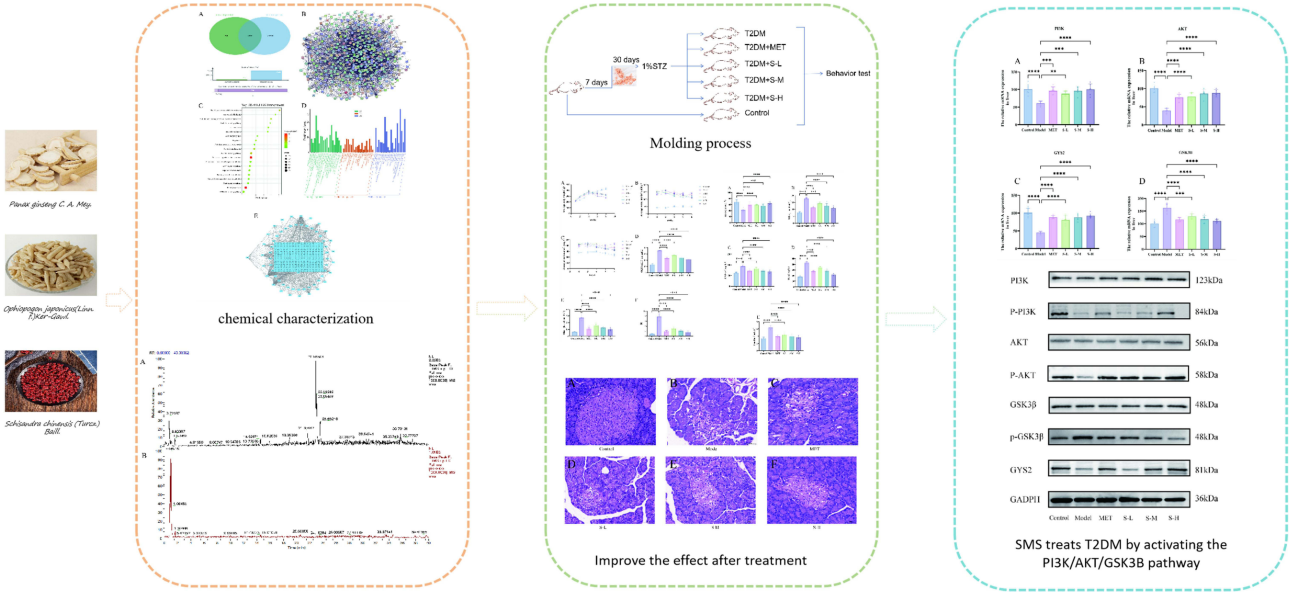

Drugs used to treat T2DM include insulin, biguanides, glucagon-like peptide-1 (GLP-1) agonists, sulfonylureas, and thiazolidinediones.[5,6] However, common side effects of biguanides include gastrointestinal issues such as nausea, indigestion, diarrhea, and lactic acidosis, with mortality rates as high as 50% if lactic acidosis occurs.[7–9] Hypoglycemia is the most serious adverse effect of insulin therapy, and severe cases can lead to headache, dizziness, confusion, coma, shock, and even death.[10] Diabetes, formerly known as "thirst disease" in ancient Chinese medical writings, has a lengthy history of treatment in traditional Chinese medicine. The "SuWen · Strange Disease" was the first to document this condition, while the "Huangdi's Internal Classic" described it as Xiaoshi, Phyrexia, or Xiaozhong based on its symptoms and pathogenesis.[11] According to traditional Chinese medicine, the primary causes of this condition are overconsumption of fatty and sweet foods, emotional disturbances, and deficiencies in the five viscera, with Yin deficiency and dry heat as the main pathogenic factors.[12] Herbal formulas such as Huangqintalishi decoction,[13] Sanhuang decoction,[14] and Wuling San[15,16] have become focal points in T2DM research. The phosphatidylinositol 3-kinase/protein kinase B/Glycogen Synthase Kinase 3 Beta (PI3K/AKT/GSK3B) signaling pathway is one of the major insulin signaling pathways, regulating processes such as cell proliferation, autophagy, and inflammation. It controls various biological processes, including cell proliferation, autophagy, and the inflammatory response. The PI3K/Akt/GSK3B signaling pathway plays a crucial role in regulating cell growth and metabolism. Activated in response to insulin, it regulates key metabolic processes, including glucose and lipid metabolism, as well as protein synthesis.

SMS comes from Medical Qiyuan written by Zhang Element in the Jin Dynasty.[17] It is composed of Panax ginseng, Ophiopogon and Schisandrae. Panax ginseng consists of the dried roots and rhizomes of *Panax ginseng* C. A. Mey., a plant of the Araliaceae family. Ophiopogon consists of the dried tuberous roots of *Ophiopogon japonicus* (L.f). Ker-Gawl, a plant of the Liliaceae family. Schisandrae consists of the dried mature fruits of *Schisandra chinensis* (Turcz). Baill., a plant of the Magnoliaceae family. It has the effect of beneficial qi and promoting fluid, restraining Yin and preventing perspiration. Ophiopogon Gan cold, nourishing Yin Qingheat, moistening lung Shengjin, as minister medicine, When Panax ginseng and Ophiopogon are used together, the benefits of invigorating qi and nourishing Yin are enhanced. Schisandric acid warm, collect lung antiperspirant, produce fluid to quench thirst, for adjuvant medicine; Three medicines used in combination, one tonifying, one moistening and one restraining, invigorating qi and nourishing Yin, promoting fluid to quench thirst, and restraining Yin and stopping perspiration.[18] This study aims to explore the

pharmacodynamic evaluation and mechanism of SMS in the treatment of T2DM, and evaluate the influence of SMS on T2DM through network pharmacology, qRT-PCR, WB and other methods, hoping to provide a new theoretical basis for the treatment of T2DM and provide theoretical support for clinical application.

Materials and Methods

Instrument

UPLC-Q-Exactive Orbitrap/MS was used for qualitative composition analysis of SMS chemical composition. KQ-250DE type CNC ultrasonic cleaner was used to promote the dissolution of drugs. The mRNA of rat liver tissue was detected by Real-time fluorescence quantitative PCR instrument. Blood glucose meter (model 2205076630, Yuyue Group), Blood glucose test paper was used to detect blood glucose in rats. The serum parameters of rats were detected by enzyme label instrument.

Drugs and Reagents

Decoction pieces of Panax Ginseng (220602), Ophiopogon (231204611), Schisandra (20230901) were purchased from Kyushu Shanghai Medical Center, Kangmei Pharmaceutical Co., LTD., Guangdong Huizun Traditional Chinese Medicine Decoction Pieces Co., LTD., Panax ginseng C.A. Mey. (Panax ginseng): The dried roots and rhizomes of Ophiopogon japonicus (L.f). Ker-Gawl (dried root tubers), and Schisandra chinensis (Turcz). Baill (dried ripe fruit). All of them are in line with the collection standards of the 2020 edition of Chinese Pharmacopoeia. The metformin-glibenclamide capsule was administered to animals as a positive control. Streptozotocin was used as a modeling agent to establish T2DM rat models by intraperitoneal injection. The antibodies PI3K, P-PI3K, AKT, P-AKT, GSK3B, GYS2, and GAPDH specifically recognize and bind to their respective target proteins, enabling detection and quantification of these proteins through various antibody combinations.

Analysis of the Chemical Constituents of the Traditional SMS Decoction

Panax ginseng, Ophiopogon and Schisandrae were mixed in a 3:3:2 ratio.[19] After dissolving 1.0 g of freeze-dried SMS in 10 mL of 50% methanol, which is equal to 0.9 g of Panax ginseng decoction pieces, 0.9 g of Ophiopogon decoction pieces, and 0.6 g of Schisandra decoction pieces, the sample was weighed. Chromatography was performed using a HALO 90A C18 column (100 mm × 2.1 mm, 2.7 μm), with a mobile phase comprising 0.1% formic acid in aqueous solution (A) and 0.05% acetonitrile solution (B). The gradient elution procedure was as follows: from 0 to 3.24 min, 5% A to 10% A; from 3.24 to 8.64 min, 10% A to 14% A; from 8.64 to 14.04 min, 14% A to 20% A; from 14.04 to 20.52 min, 20% A to 40% A; from 20.52 to 24.84 min, 40% A to 42% A; from 24.84 to 28.08 min, 42% A to 44% A; from 28.08 to 32.40 min, 44% A to 60% A; from 32.40 to 34.56 min, 60% A to 62% A; and from 34.56 to 40.0 min, 62% A to 80% A. The column temperature was maintained at 30 °C, the sample volume was 3 μL, and the flow rate was 0.3 mL/min. Electrospray ionization (ESI) was used in both positive and negative ion monitoring modes. For positive and negative modes, the spray voltage was +3.3 kV and −2.6 kV, respectively. In addition to keeping the ion transfer tube temperature at 320°C, the auxiliary gas flow rate was set at 3 mL/min. The Full MS/dd-MS2 scanning mode had a Full MS resolution of 70,000 and a dd-MS2 resolution of 17,500. The scanning quality range was m/z 80–1200.

Network Pharmacology and Molecular Docking

Establishment of the Active Ingredient and Disease Target Database

The compounds obtained from mass spectrometry analysis were imported into the TCM System Pharmacology Technology platform database (TCMSP, http://tcmspw.com/tcmsp.php). [20] The category was set to "Chemical name" to specifically search for related active ingredients. The SMILES names of the retrieved active ingredients were then input into SwissTargetPrediction (http://www.swisstargetprediction.ch/)[21] selecting the species "Homo sapiens" to obtain the gene targets corresponding to the active ingredients, thereby establishing the active ingredient target database. To locate disease targets, we utilized the Disgenet database (https://www.disgenet.com)[22] and the GeneCards database (https://www.genecards.org/). [23] Using "type 2 diabetes" as a keyword, we searched for and screened disease gene

targets related to type 2 diabetes from these databases. Finally, the disease targets and active ingredient targets were imported into Venny2.1.0 (https://bioinfogp.cnb.csic.es/tools/venny/index.html) to obtain the intersection of the two target sets, thus creating an intersection target database.

Construction of the PPI Core Network Structure Diagram

To further explore the interaction mechanisms of the active ingredients in SMS for the treatment of diabetes mellitus, the obtained intersection targets were imported into the STRING database (https://cn.string-db.org/). The analysis was conducted using "Homo sapiens" as the selected species to construct the PPI target interaction network diagram.

GO and KEGG Pathway Analysis of Intersection Targets

The overlapping gene targets will be input into the DAVID database (https://david.ncifcrf.gov/)[24] for GO enrichment analysis of biological processes and KEGG pathway analysis. The results will then be analyzed using the "Micro Letter" website (https://www.bioinformatics.com.cn) to create pillar charts and bubble charts for visualization.

Screening of Core Compounds

A total of 39 compounds in SMS were identified using UPLC-Q-Orbitrap/MS. These identified compounds were selected as the primary subjects for network pharmacological analysis and were imported into Cytoscape 3.9.0, along with the associated cross-targets, for interaction network analysis. The degree of interaction for each compound with the gene targets was assessed based on the number of associated targets.

Molecular Docking and Visualization

This study investigated the mechanism of action of SMS on the PI3K/AKT pathway. We selected four key active factors (PI3K, AKT1, GSK3B, GYS2) involved in this pathway and collected relevant small molecule and protein information from the PDB database (https://www1.rcsb.org/). For molecular docking, AutoDock Vina software was employed after performing energy minimization on the small molecule ligands and receptor proteins. Based on binding energy references, we screened combinations of small molecules and proteins with low binding energy. Finally, PyMOL 2.5.0 software was used to visually present the docking results.

Verification of Animal Experiments

Preparation of Drug Solution

Weigh 48.6 g of Panax ginseng, 48.6 g of Ophiopogon, and 32.4 g of Schisandra chinensis. After grinding through a No. 2 sieve, mix the powders evenly and place them into a decoction pot with 2000 mL of distilled water. Boil for 1 hour, then drain the hot liquid. The filtrate was distilled at 70°C and concentrated to volumes of 600 mL, 300 mL, and 150 mL, respectively. Finally, the concentrated solutions were removed, refrigerated, and sealed at a low temperature of 4°C.

Experimental Animals

Beijing Huafukang Biotechnology Co., Ltd. (SCXK Jing 2019–0008) was the source of sixty 6-week-old SPF SD rats, each weighing 200 ± 10 g. The rats were housed in a controlled environment at the Laboratory Animal Center of Shandong University of Traditional Chinese Medicine, maintained at a temperature of 18 to 25°C, with a relative humidity of 50% to 60%. A 12-hour cycle of light and dark was applied to them. All procedures complied with the ethical standards of animal experimentation established by Shandong University of Traditional Chinese Medicine (License No. 110322241100935627). Metformin (MET) at 0.45 $mg{\cdot}kg^{-1}$ was one of the treatments, along with SMS at low dose (2.16 $g{\cdot}kg^{-1}$), middle dose (4.32 $g{\cdot}kg^{-1}$), and high dose (8.64 $g{\cdot}kg^{-1}$).

Modeling and Grouping of Experimental Animals

SD rats were randomly assigned to six groups following seven days of adaptive feeding: model, positive drug (Met), SMS low-dose (S-L), medium-dose (S-M), high-dose (S-H), and normal control (Control). Each group, except the Control, was assigned a unique identifier. The non-Control groups were fed a high-fat diet. After 4 weeks on the high-fat diet, these groups received a single intraperitoneal injection of 2% streptozotocin solution (30 mg kg-1), prepared

immediately. The streptozotocin was wrapped in ice in tin foil, stored away from light, and prepared in an ice bath with a 0.1 mol/L citric acid-sodium citrate buffer (pH 4.5), with an injection volume of 1 mL per 100 g of body weight. Three days post-injection, rats exhibiting fasting blood glucose (FBG) levels greater than 11.10 mmol/L, along with signs of hyperglycemia, polydipsia, polyuria, and weight loss, were considered successfully modeled.[25]

Overall Condition of the Animals

Following the completion of modeling, the rats' weights were measured weekly, and changes in weight were observed. The prescribed amounts of feed and water were administered over 24 hours, and food intake and water consumption were recorded. Random blood glucose and fasting blood glucose (after 12 hours of fasting) were measured weekly for each group. Blood samples were collected from the tail vein using a blood glucose meter and test strips, with glucose levels recorded as follow-up indices. The day before dissection, each group of rats received a 5% glucose solution (2 $g \cdot kg^{-1}$) based on body weight. At 30-, 60-, 90-, and 120-minute intervals, blood glucose levels were monitored, and variations in blood glucose levels throughout time were noted and recorded.

Enzyme-Linked Immunosorbent Assay (ELISA)

During the dissection of the rats, livers were collected from each group, frozen in liquid nitrogen, and stored at −80°C. Blood was drawn from the abdominal aorta, allowed to stand for 4 hours, and centrifuged at 8000 $r \cdot min^{-1}$ for 10 minutes. The supernatant was collected and stored at −80°C. Using an enzyme-linked immunosorbent test, serum TG, TC, HDL-C, LDL-C, MDA, SOD, Fins, TNF-α, and IL-6 were analyzed.

Histopathological Analysis of Pancreas

Each group's pancreatic tissues were gathered and preserved in 4% paraformaldehyde. To observe pancreatic morphology, paraffin slices were produced, stained with hematoxylin-eosin (HE), and seen under a light microscope.

Quantitative Real-Time PCR Analysis

Total liver RNA was extracted using the Flying Shark Plus tissue RNA extraction kit, and cDNA was synthesized with Rescript II RT SuperMix for quantitative PCR (qPCR). qPCR was conducted using a fluorescent quantitative PCR apparatus and 2×SYBR Premix UrTaq® II. The relative expression of mRNA was normalized to the housekeeping gene β-actin and calculated using the $2^{-\Delta\Delta Ct}$ method. Suzhou Jinweizhi Biotechnology Co., Ltd. produced the primers used in this investigation. Primer design details are provided in Table 1.

Western Blot

Liver tissue was treated with RIPA lysate, thoroughly ground using a freezer mill, and the supernatant was collected. Protein concentration was quantified using a BCA assay, and then the proteins were denatured. Proteins were transferred to a PVDF membrane after being separated using 10% SDS-PAGE. 5% BSA was used to block the membrane for two hours at room temperature. The following primary antibodies were applied at a 1:5000 dilution and incubated overnight at 4°C: PI3K, P-PI3K, AKT, P-AKT, GSK3B, and P-GSK3B. Three TBST washes of the membrane were performed the

Table 1 Information for Primer Sequence

Target	Direction	Sequence
PI3K	Forward	5'-TACTGCGTGGCAACCTTTATC-3'
	Reverse	5'-GCTGTCCGTCATCTTTCACCA-3'
AKT1	Forward	5'-TACGGTGCGGAGATTGTGTC-3'
	Reverse	5'-ACAGCCCGAAGTCCGTTATC-3'
GSK3b	Forward	5'-TCCGAGGAGAGCCCAATGTT-3'
	Reverse	5'-CGTGTAATCGGTGGCTCCAA-3'
GYS2	Forward	5'-GAGTTTGTCCGAGGCTGTCA-3'
	Reverse	5'-GTTCGTAGTCACACTGGGGAT-3'
β-action	Forward	5'-CTCTGTGTGGATTGGTGGCT-3'
	Reverse	5'-CGCAGCTCAGTAACAGTCCG-3'

https://doi.org/10.2147/DMSO.S507953

next day. After adding a diluted 1:500 secondary antibody, the mixture was shaken and allowed to sit at room temperature for an hour. The membrane was coated with a supersensitive luminous solution for chemiluminescence detection following three TBST washes. ImageJ software was used to assess the target bands' gray levels.

Statistical Analysis

The data was analyzed using GraphPad Prism (version 10.1, GraphPad, United States), and the mean ± standard deviation is the outcome. A one-way analysis of variance (ANOVA) was performed to assess the differences between the groups, followed by LSD post hoc analysis to identify specific group differences. There was a significant difference when the result was *P < 0.05, and the significance of the difference progressively increased as **P < 0.01, ***P < 0.001, and ****P < 0.0001.

Results

Analysis of UPLC-MS/MS and Screening of Active Ingredients

Based on ion fragment data from literature, 39 components were identified in SMS using UPLC-Q-Orbitrap/MS. These consist of 17 components from the five-flavor category, 4 from Ophiopogon, and 25 from Panax ginseng. Detailed compound information and the total ion chromatogram are presented in Figure 1A and B and Table 2. To find the matching targets of the active components, the discovered compounds were entered into the SwissTargetPrediction and TCMSP databases. A total of 23 active ingredients were screened, leading to the establishment of an active ingredient database for SMS.

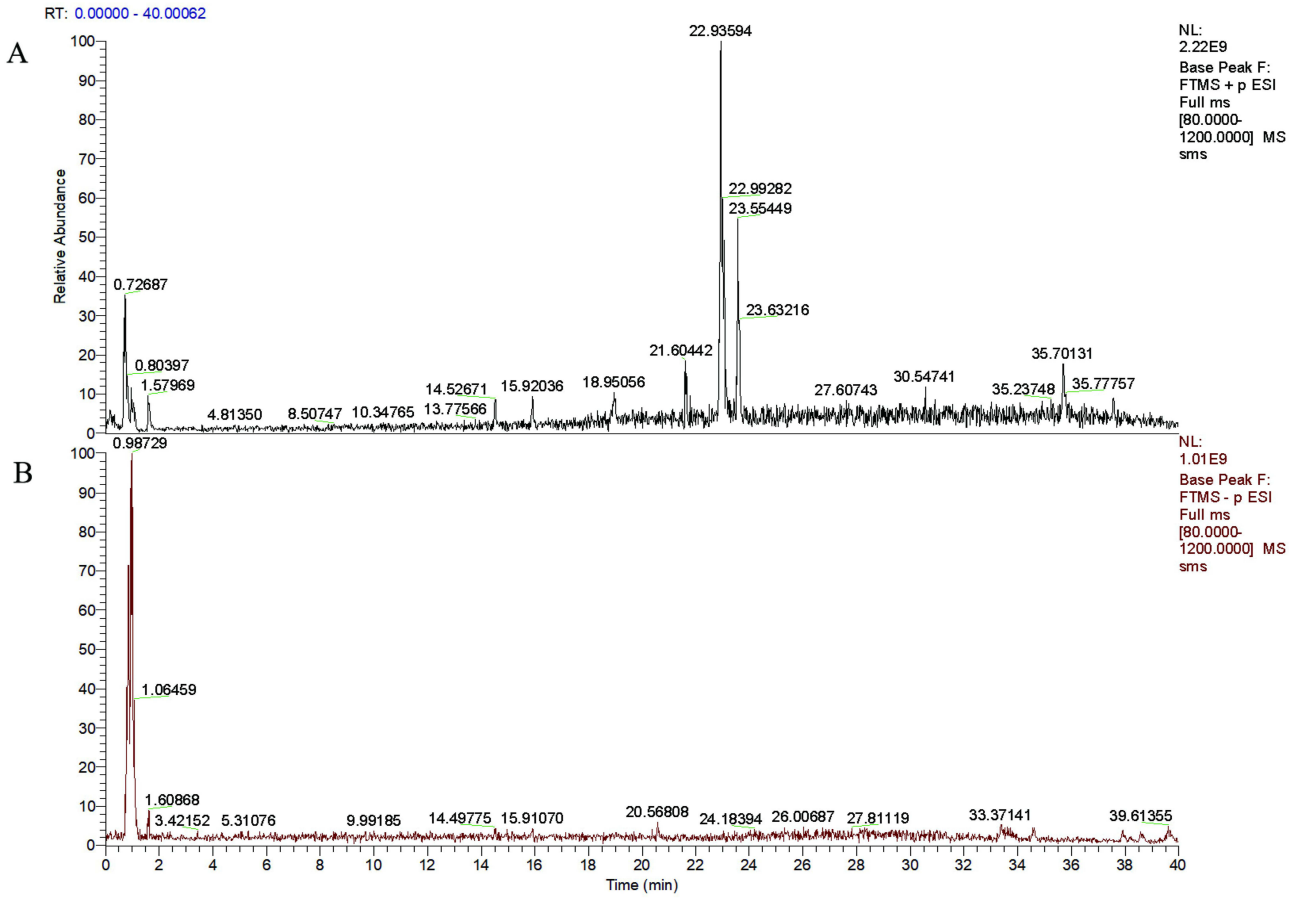

Figure 1 Total ion chromatogram of SMS traditional decoction in both positive and negative ion modes. (**A**) Positive modes. (**B**) Negative modes.

Table 2 Identification of Chemical Constituents in SMS

Number	Identification	Formula	Rt (min)	Quasi-molecular ion	Error (ppm)	Measured value	Calculated value	Major Fragments	Source
1	Caffeic acid	C9H8O4	1.17	[M−H]−	8.7	179.0365	179.0351	101.0241, 89.0240	BC
2	Protocatechuic acid	C7H4O4	2.61	[M−H]−	7.26	153.0187	153.0182	109.0290, 135.0368, 61.9880	ABC
3	TryptopHan	C11H12N2O2	3.12	[M+H]+	1.22	205.0974	205.0972	188.07098, 146.06030, 159.09186	ABC
4	Schindilactone C or isomer	C29H36O11	12.27	[M−H]−	1.96	559.21849	559.22	541.21198, 365.13647	C
5	Azelaic Acid	C9H16O4	13.52	[M−H]−	0.29	187.0965	187.0976	141.86751, 125.09663	BC
6	Ginsenoside Rg1	C42H72O14	19.51	[M+HCOO]-	−1.91	845.4877	845.4893	799.48218, 637.42932, 475.37769, 391.28354	A
7	24(R)-pseudoginsenoside F11	C42H72O14	19.6	[M+HCOO]-	−1.91	845.4877	845.4893	799.48154, 653.42175	A
8	Ginsenoside Rf	C42H72O14	19.7	[M+HCOO]-	−1.91	845.4877	845.4893	799.48242, 637.4269, 475.37756, 391.28381	A
9	notoginsenoside R2	C41H70O13	19.9	[M+HCOO]-	−1.66	815.4774	815.4788	769.47095, 637.42896, 475.37769	A
10	Floralginsenoside F	C42H72O15	19.9	[M-H]-	−2.99	815.4774	815.4798	637.43048, 475.37775	A
11	Ginsenoside F5	C41H70O13	19.91	[M+HCOO]-	−1.47	815.4775	815.4787	769.47198, 637.66321, 475.79550, 391.83475	A
12	Pseudoginsenoside Rt3	C41H70O13	20.05	[M+HCOO]-	−1.55	815.5477	815.4787	769.47272, 607.24796	A
13	Ginsenoside Rg3	C42H72O13	20.24	[M+HCOO]-	−1.81	829.4929	829.4944	637.42957, 475.37726	A
14	Ginsenoside F1	C36H62O9	20.34	[M+HCOO]-	−6.86	683.4356	683.4365	637.42664, 475.37836, 391.28546	A
15	Ginsenoside F3	C41H70O13	20.45	[M+HCOO]-	−2.15	815.477	815.4787	621.19965, 391.83456	A
16	Ginsenoside Rh1	C36H62O9	20.63	[M+HCOO]-	−1.74	683.4353	683.4365	637.42242, 475.37851, 391.28391	A
17	Ginsenoside Ro	C48H76O19	20.69	[M-H]-	−4.04	955.4869	955.4908	793.43518, 613.37262, 569.38196, 455.39141	A
18	Chikusetsusaponin IVa	C42H66O14	21.48	[M-H]-	−4.15	793.4347	793.438	631.38153, 569.38306, 455.35342	A
19	Zingibroside R1	C42H66O14	21.58	[M-H]-	−1.68	793.4367	793.438	631.38379, 569.38129, 455.35333	A
20	Meprednisone acetate or isomer	C24H30O6	22.15	[M+H]+	0.23	415.2116	415.2115	415.21161, 415.21161, 353.17944	AC
21	Ginsenoside Rg9	C42H70O13	22.68	[M+HCOO]-	1.57	827.4787	827.4774	781.47266, 619.41870	A
22	Ginsenoide Rg6	C42H70O12	23.57	[M+HCOO]-	0.46	811.4842	811.4838	765.48010, 619.41937	A
23	SchisandrolA	C24H32O7	23.62	[M+H]+	0.52	433.2184	433.2221	415.21298, 400.18991, 358.13977	C

(*Continued*)

https://doi.org/10.2147/DMSO.S507953

https://doi.org/10.2147/DMSO.S507953

Table 2 (Continued).

Number	Identification	Formula	Rt (min)	Quasi-molecular ion	Error (ppm)	Measured value	Calculated value	Major Fragments	Source
24	Gomisin J	C22H28O6	23.68	[M+H]+	−4.95	389.1939	389.1959	325.14334, 287.09113, 227.07085	C
25	Rubrisandrins A or isomer	C22H28O6	23.79	[M+H]+	−7.7	389.1929	389.1959	373.09348, 356.18799	C
26	Ginsenoside F4	C42H70O12	23.94	[M+HCOO]-	0.46	811.4842	811.4838	765.47552, 619.41504	A
27	Allyl 2-O-benzoyl-3- O-benzyl-6-deoxy-α-L-mannopyranoside or isomer	C23H26O6	25.77	[M+H]+	0.14	399.1803	399.1802	368.16238, 330.11029, 315.08643	AC
28	Ginsenoside Rg2	C42H72O13	26.58	[M+HCOO]-	−1.71	829.493	829.4944	783.63761, 391.83542	A
29	Ginsenoside F2	C42H72O13	27.21	[M+HCOO]-	−1.81	829.4929	829.4944	783.48737, 621.43512, 459.38348, 375.29126	A
30	Gedunin or isomer	C28H34O7	27.83	[M+H]+	4.118	483.2397	483.2377	437.19763, 414.16827, 381.13687	A
31	Rubschisandrin or isomer	C23H28O6	29.39	[M+H]+	3.43	401.1972	401.1959	370.17783, 355.15442, 323.12802	C
32	Gomisin K2 or isomer	C23H30O6	32	[M+H]+	0.95	403.2125	403.2115	371.18665, 301.10782, 287.09198	C
33	Ginsenoside Rg5	C42H70O12	32.48	[M+HCOO]-	−1.36	811.4827	811.4838	765.47711, 545.77991, 439.81604	A
34	Gomisin G	C30H32O9	32.8	[M+H]+	−4.19	537.2097	537.2119	371.14948, 343.11618, 285.07559	C
35	Schisanhenol	C23H30O6	33.09	[M+H]+	1.14	403.2127	403.2115	357.17029, 325.14349	C
36	Isomer of schisantherin A	C30H32O9	33.25	[M+H]+	−2.49	537.2106	537.2119	312.09946, 343.11667	C
37	Schisandrin A or isomer	C24H32O6	35.71	[M+H]+	3.679	417.2287	417.2272	316.13107, 301.10748, 285.11267	C
38	Gomisin N	C23H28O6	37.57	[M+H]+	2.95	401.1971	401.1959	386.17307, 371.18790, 356.16428	C
39	Schisandrin B or isomer	C23H28O6	37.76	[M+H]+	0.36	401.196	401.1959	386.17377, 301.10678, 331.11768, 227.07147	C

Notes: A represents Panax ginseng, B represents Ophiopogon, and C represents Schisandra.

Network Pharmacologyanalysis Results

Identification of Common Targets

A total of 417 active ingredient targets associated with SMS and 7548 disease targets related to type 2 diabetes were collected. These targets were analyzed using the Venny 2.1.0 tool to identify common targets, resulting in 359 intersection targets (Figure 2A). An intersection target database was subsequently established.

PPI Interaction Network Diagram

There were 5521 edges and 359 nodes in the PPI protein interaction network diagram that was created. The average node degree was 30.8, and the average local clustering coefficient was 0.486. 2431 was the anticipated number of edges. The degree values were used as evaluation criteria to rank the targets. It was found that TNF (degree=176), STAT3 (degree=141), and GSK3B (degree=102) exhibited high degree values (Figure 2B), suggesting that these targets may be key for the treatment of type 2 diabetes.

Drug Component-Gene Interaction Network

A total of 23 compounds and their corresponding intersecting gene targets were imported into Cytoscape 3.9.0 for gene interaction network analysis (Figure 2C). Schisandrol A was selected as a key compound based on the number of targets

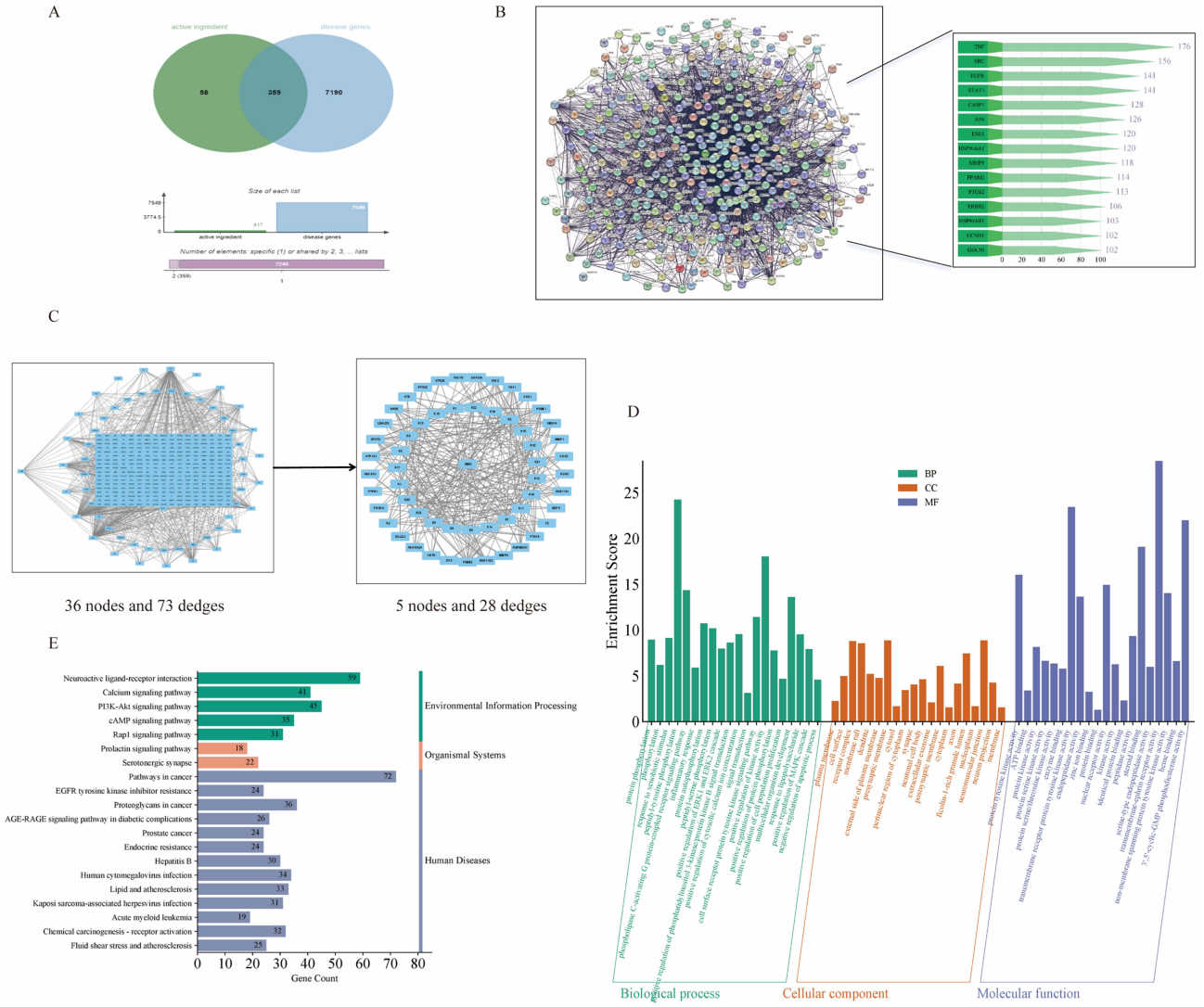

Figure 2 (**A**) Network pharmacology predicts SMS therapeutic pathway for type 2 diabetes. Acquisition of intersection targets. (**B**) PPI interaction network diagram. (**C**) Drug composition - Gene target Network. (**D**) GO enrichment map. (**E**) KEGG enrichment map.

https://doi.org/10.2147/DMSO.S507953

Table 3 Drug Component-Gene Interaction Network

CAS	Label	Identification	Number of Targets
62956–48-3	R20	Gomisin G	119
7432–28-2	R23	SchisandrolA	114
61281–38-7	R22	Schisandrin A or isomer	113
123–99-9	R17	Azelaic Acid	61
331–39-5	R16	Caffeic acid	50
54–12-6	R14	TryptopHan	49
80418–25-3	R15	notoginsenoside R2	40
51415–02-2	R3	Chikusetsusaponin IVa	38
63223–86-9	R2	Ginsenoside Rh1	36
80930–74-1	R4	Zingibroside R1	32
98474–75-0	R7	Pseudoginsenoside Rt3	27
11019–45-7	R10	Ginsenoside Rg3	24
53963–43-2	R1	Ginsenoside F1	23
52286–74-5	R9	Ginsenoside Rg2	22
22427–39-0	R12	Ginsenoside Rg1	21
62025–49-4	R11	Ginsenoside F2	21
52286–58-5	R13	Ginsenoside Rf	20
189513–26-6	R6	Ginsenoside F5	20
62025–50-7	R8	Ginsenoside F3	16
74964–14-0	R5	Ginsenoside Rg5	13
69363–14-0	R21	Schisanhenol	3
61281–37-6	R19	Schisandrin B or isomer	2
69176–52-9	R18	Gomisin N	2

associated with the intersecting genes, along with its characteristics and significance in drug development. Ginsenoside Rg3, Ginsenoside Rg5, Ginsenoside F2, Ginsenoside F3, and Schisandrin B (or its isomer) were identified as core components for subsequent molecular docking analysis (Table 3). The purpose of this investigation was to look into how these substances affected the PI3K/AKT pathway.

Results of GO and KEGG Enrichment Analysis

To further explore the specific mechanism of action of the active ingredients in SMS for treating type 2 diabetes, we conducted GO (Figure 2D) and KEGG (Figure 2E) enrichment analyses on cross genes. KEGG enrichment analysis focuses on identifying biological signaling pathways associated with drug targets, providing a more intuitive understanding of the pathways through which the drug exerts its efficacy. Analysis of the enrichment results, presented as horizontal bar graphs, revealed that SMS drug targets were strongly associated with classical neural activity and cancer pathways, as well as with significant enrichment in the PI3K/AKT pathway, calcium ion signaling pathway, and cAMP signaling pathway. These findings provide a basis for further investigation into the mechanism of action of SMS, suggesting that SMS may modulate its function by regulating factors within the PI3K/AKT pathway, thereby playing a pharmacological role in treating T2DM. GO enrichment analysis revealed that the active components of SMS are primarily associated with biological processes (BP) such as tyrosine phosphorylation and the activation of the G protein-coupled receptor signaling pathway mediated by phospholipase C. Regarding molecular function, the main activities influenced by Shengmai SAN include transmembrane receptor protein tyrosine kinase activity and 3', 5'-cyclic GMP phosphodiesterase activity. Cell composition (CC) analysis indicated that the drug components may interact with receptor complexes and membrane rafts on the cell membrane to exert their pharmacological effects. These findings are reflected in the PI3K/AKT signaling pathway transduction process, further suggesting that Shengmai SAN may exert its pharmacological effects through modulation of the PI3K/AKT pathway.

Table 4 Molecular Docking Results and Visualization

Name	Receptor Protein	Small Ligand Molecules	Binding energy kj/mol
PI3K	1E8Y	Ginsenoside F3	−9.1
GSK3B	3SAY	Ginsenoside Rg5	−9.9
GSK3B	3SAY	Ginsenoside Rg3	−10.1
GSK3B	3SAY	Ginsenoside F3	−9.8
AKT	8R5K	Ginsenoside Rg3	−8.9
GSK3B	3SAY	Schizandrin	−7.5
AKT	4EJN	Ginsenoside Rg3	−8.4

Molecular Docking and Visualization Results

We selected receptor proteins related to the PI3K/AKT pathway, including PI3K (1E8Y, 2RED), AKT1 (4EJN, 8R5K), and GSK3B (3I4B, 4J7I, 3SAY), and used AutoDock Vina software to conduct molecular docking with the core components identified from the screening. The docking results with lower binding affinities, as shown in Table 4, were visualized using PyMOL 2.5.0 to highlight the specific binding sites and hydrogen bond lengths (Figure 3A-D). Based on the molecular docking results, we preliminarily conclude that certain components of SMS can easily and stably bind to proteins within the PI3K/AKT pathway, thereby influencing its activity.

Experimental Verification

The Effect of SMS on the General Condition of T2DM Rats

The results showed that, compared to the blank group, rats in the model group exhibited significant weight loss (Figure 4A) along with increased food (Figure 4B) and water intake (Figure 4C), consistent with the typical "three

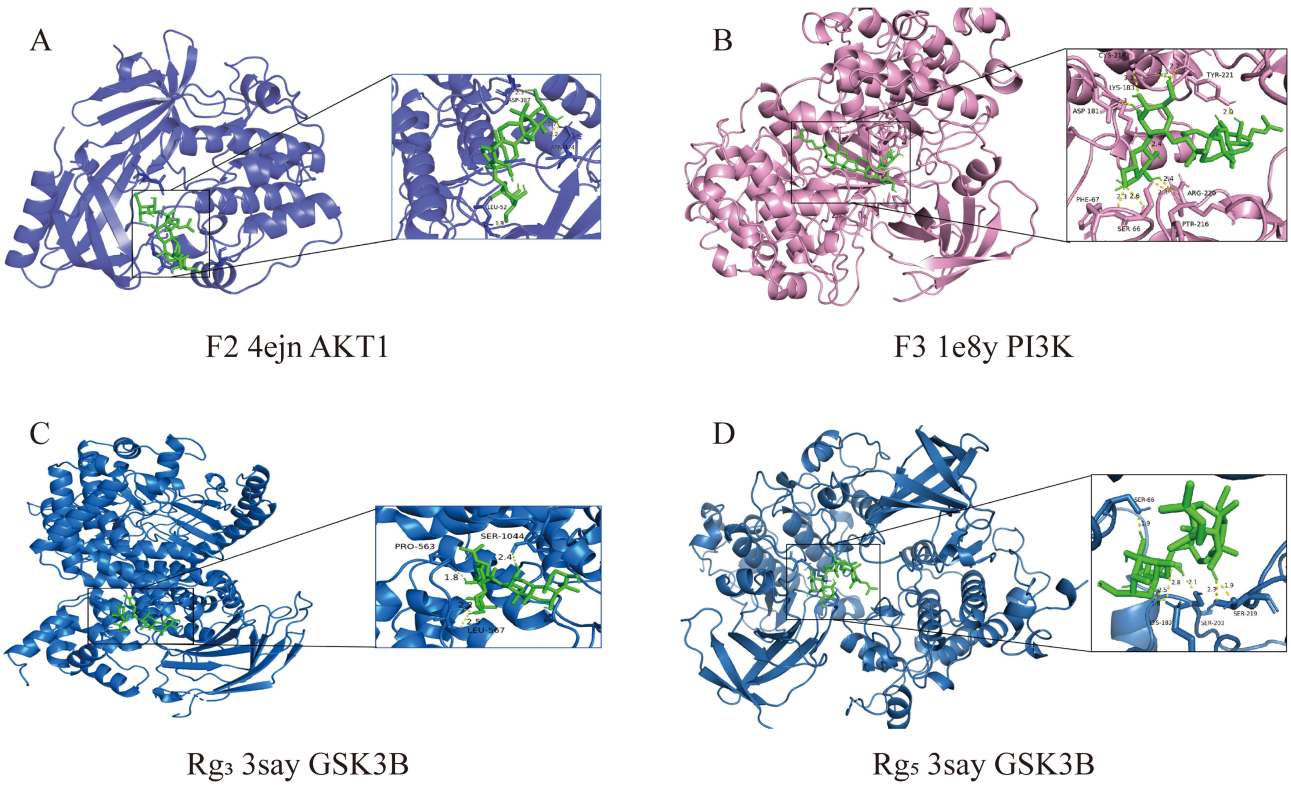

Figure 3 Molecular docking and visualization. (**A**) Docking results of ginsenoside F2 and 4EJN protein. (**B**) Docking results of ginsenoside F3 and 1E8Y protein. (**C**) Docking results of ginsenoside Rg3 and 3say protein. (**D**) Docking results of ginsenoside Rg5 and 3say protein.

https://doi.org/10.2147/DMSO.S507953

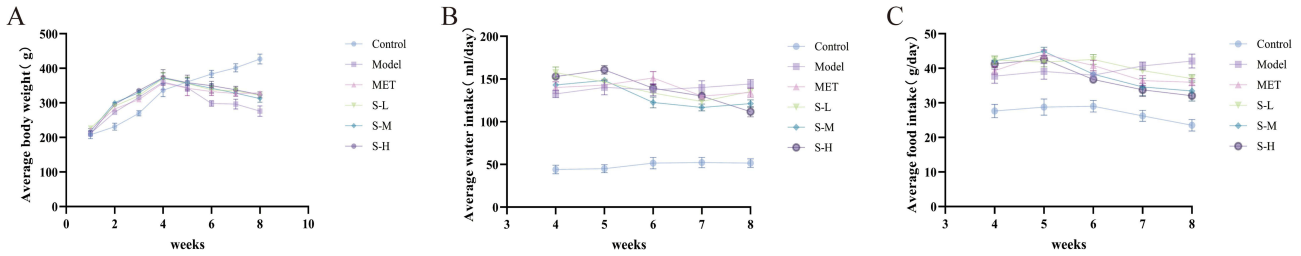

Figure 4 Effects of SMS on the General Condition of Type 2 Diabetes Mellitus (T2DM) Rats. (**A-C**) Changes in average body weight (**A**), food intake (**B**), and water intake (**C**) of rats in each group following drug treatment.

more and one less" symptoms of T2DM. Following SMS administration, the symptoms were significantly improved in both the MET and SMS-treated groups, with the most notable improvement observed in the SMS high-dose group.

Effect of SMS on Lipid Metabolism

Compared to the normal control group, the serum total TC levels in the model group were increased (***P < 0.001), while the TG and LDL-C levels were significantly elevated (****P < 0.0001), and HDL-C levels were significantly reduced (****P < 0.0001). These results indicate that the model group rats exhibited signs of lipid metabolism disorder. Compared to the model group, TC levels in the SMS treatment groups were reduced (***P < 0.001); TG and LDL-C levels were significantly lowered (****P < 0.0001), while HDL-C levels were significantly increased (****P < 0.0001). The improvement was most pronounced in the SMS high-dose administration group (Figure 5A-D). These findings suggest that SMS can reduce blood lipids and improve lipid metabolism disorders in rats.

Effects of SMS on Serum Inflammatory Factors and Oxidative Stress in Rats

The model group had considerably higher blood levels of MDA, tumor necrosis TNF-α and IL-6 compared to the normal control group (****P < 0.0001), but lower serum levels of SOD (****P < 0.0001). This indicates the presence of oxidative stress and inflammation in the model group. In comparison to the model group, the levels of MDA, TNF-α and IL-6 in the SMS treatment group were significantly decreased (****P < 0.0001), while SOD levels were significantly increased (****P < 0.0001). The SMS high-dose group exhibited greater improvement than the MET group (Figure 6A-D). These data imply that SMS can help with oxidative stress and inflammation.

The Effect of SMS on Blood Glucose Regulation

Compared to the normal control group, the model group showed significantly elevated blood glucose, glucose tolerance, insulin resistance (IR), and insulin levels (****P < 0.0001), confirming that blood glucose regulation was disrupted and the model was successfully established. Compared to the model group, the SMS administration group exhibited significant reductions in blood glucose, glucose tolerance, IR, and insulin levels (****P < 0.0001), with the SMS high-

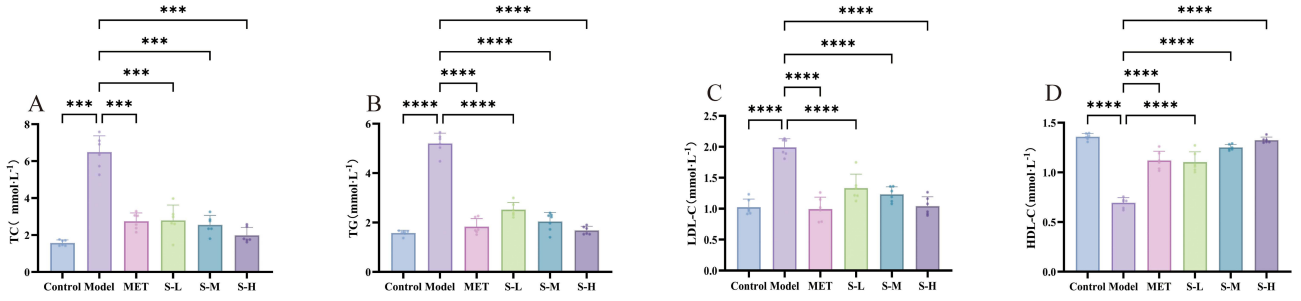

Figure 5 Effects of SMS on Lipid Metabolism. (**A-D**) After the action of the drug, the changes in the blood lipid level of each group of rats. (**A**) The expression results of TC. (**B**) The expression results of TG. (**C**) The expression results of LDL-C. (**D**) The expression results of HDL-C.****P* < 0.001 and *****P*<0.0001 vs Control group; ****P* < 0.001 and *****P*<0.0001 vs Model group.

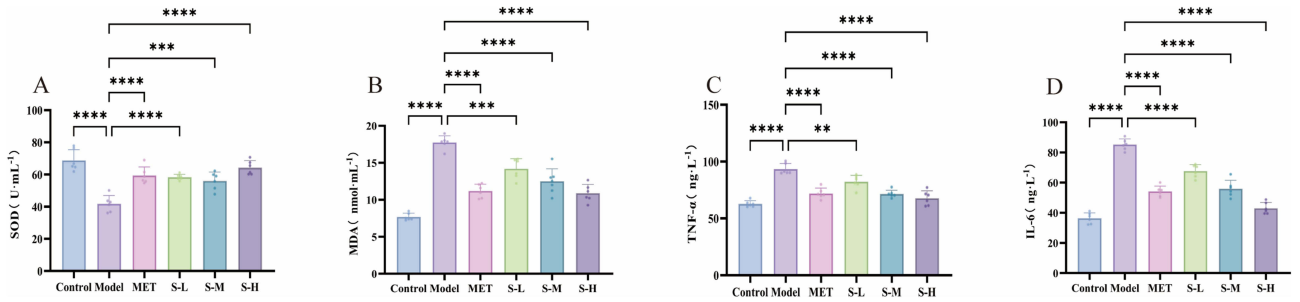

Figure 6 Effect of SMS on serum parameters of type 2 diabetic rats. (**A**) The expression results of SOD. (**B**) The expression results of MDA. (**C**) The expression results of TNF-α. (**D**) The expression results of IL-6. ****P<0.0001 vs Control group; **P < 0.01, ***P < 0.001 and ****P<0.0001 vs Model group.

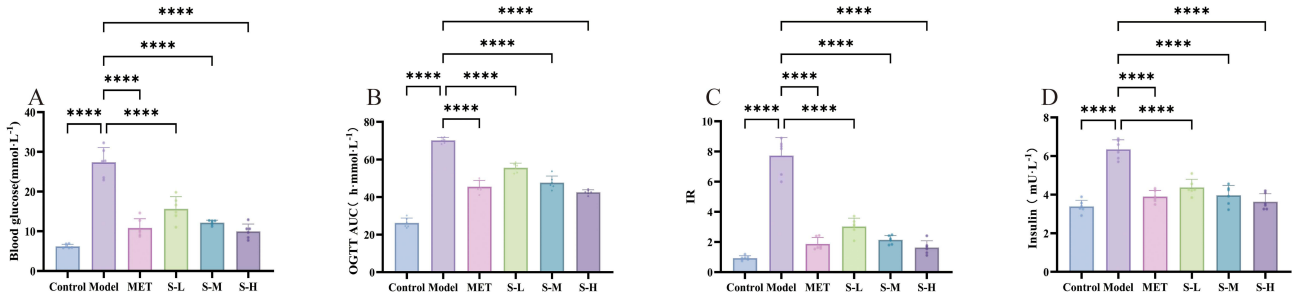

Figure 7 Changes in blood glucose levels in each group of rats after drug treatment. (**A**) Representing fasting blood glucose. (**B**) Representing glucose tolerance. (**C**) representing IR. (**D**) representing the insulin content. ****P<0.0001 vs Control group; ****P<0.0001 vs Model group.

dose group showing greater improvement than the MET group (Figure 7A-D). These results suggest that SMS can help regulate blood glucose disorders in the treatment of T2DM.

Effects of SMS on Pancreatic Histopathology in Type T2DM Rats

Staining results indicated that the volume of pancreatic islet tissue was larger in the normal control group. The interstitial tissue appeared loose, and the cytoplasm was well-defined. No signs of cell atrophy, vacuolation, or other abnormalities were observed, indicating normal islet tissue morphology. In contrast to the normal control group, islet cells in the model group exhibited denaturation, necrosis, fibrous tissue hyperplasia, significant alterations in fibroblast morphology, and a marked decline in function. Compared to the model group, cells in the high-dose administration group showed slight deformation and necrosis without evidence of exocrine gland invasion. Morphological and functional improvements in the islets were observed, suggesting that high-dose SMS provides a better protective effect on pancreatic tissue (Figure 8A-F).

Effects of SMS on mRNA Expression of PI3K/AKT Pathway-Related Genes in the Liver of T2DM Rats

Compared to the normal control group, the relative mRNA expressions of PI3K, AKT, and GYS2 in the liver of the model group were significantly decreased (****P < 0.0001). In comparison to the model group, the relative mRNA expressions of PI3K, AKT, and GYS2 in the SMS and metformin groups were significantly upregulated (****P < 0.0001). The results shown suggest that SMS can slightly raise the expression levels of PI3K, AKT, and GYS2 mRNA in the liver of rats. The model group showed considerably higher levels of GSK3B mRNA expression in the liver compared to the normal control group (****P < 0.0001). In comparison to the model group, the relative expression level of GSK3B mRNA in the liver of the SMS and metformin groups was significantly decreased (****P < 0.0001). The results shown suggest that SMS can reduce the expression level of GSK3B mRNA in the liver of rats to a certain extent (Figure 9A-D).

Effects of SMS on PI3K/AKT Pathway-Related Protein Expression in the Liver of T2DM Rats

P-PI3K, P-AKT, and GYS2 protein expressions were markedly lower in the model group's liver tissue than in the normal control group (*P < 0.05). In contrast to the model group, the protein expressions of P-PI3K, P-AKT, and GYS2 in the

https://doi.org/10.2147/DMSO.S507953

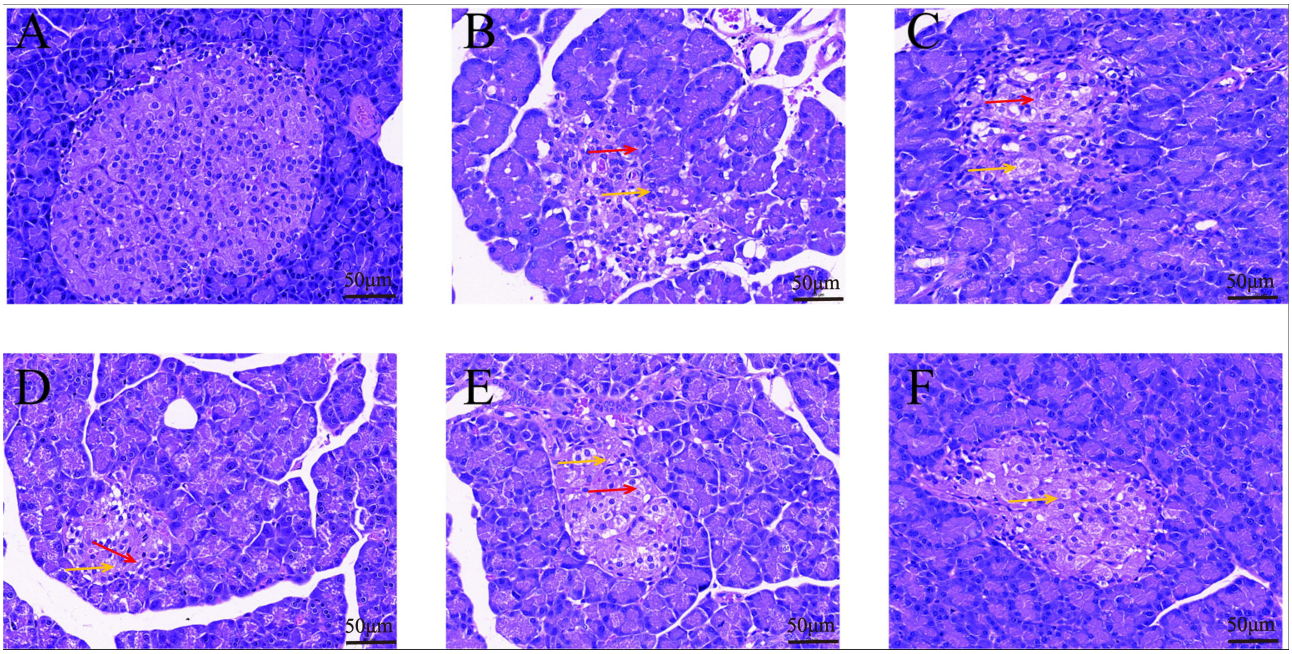

Figure 8 Effects of SMS on Pancreatic Morphology in Diabetic Rats. (**A**) Control. (**B**) Model. (**C**) MET. (**D**) S-L. (**E**) S-M. (**F**) S-H. (×400, Measuring scale: 50 μm).(↑) stands for cellular degeneration; (↑) stands for fibrous hyperplasia.

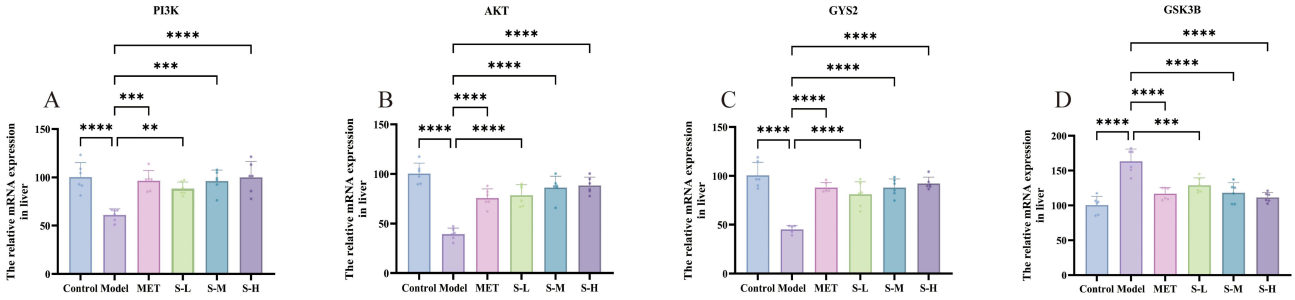

Figure 9 Effects of SMS on mRNA Expression of PI3K/AKT Pathway-Related Genes in the Liver of Type 2 Diabetes Mellitus (T2DM) Rats. (**A**) Relative mRNA level of PI3K. (**B**) Relative mRNA level of AKT. (**C**) Relative mRNA level of GYS2. (**D**) Relative mRNA level of GSK3B. ****P<0.0001 vs Control group; **P < 0.01, ***P < 0.001 and ****P<0.0001 vs Model group.

high-dose SMS group were significantly increased (*P < 0.05). Compared to the normal control group, glycogen synthase kinase 3 beta (GSK3B) protein expression in the liver tissue of the model group was significantly increased (*P < 0.05). In comparison to the model group, GSK3B protein expression in the high-dose SMS group was significantly decreased (*P < 0.05). Following PI3K phosphorylation, phosphatidylinositol (PIP3) is generated, promoting AKT activation and resulting in P-AKT production. P-AKT inhibits GSK3B activity by activating it to produce P-GSK3B, thereby reducing GSK3B's inhibition of GYS2 and promoting glycogen synthesis. Thus, non-phosphorylated PI3K, AKT, and GSK3B did not significantly vary in the model group from the normal control group. Also, there was not a big difference between the model group and the group that received SMS in the amounts of non-phosphorylated PI3K, AKT, and GSK3B (Figure 10A-G).

Discussion

The chronic metabolic condition known as T2DM is mostly brought on by insulin resistance and decreased insulin production.[26] Impaired insulin secretion is linked to dysfunction of pancreatic β cells. The liver, as the primary site of glucose and lipid metabolism, plays a key role in metabolic disorders caused by impaired IR and insulin secretion, which

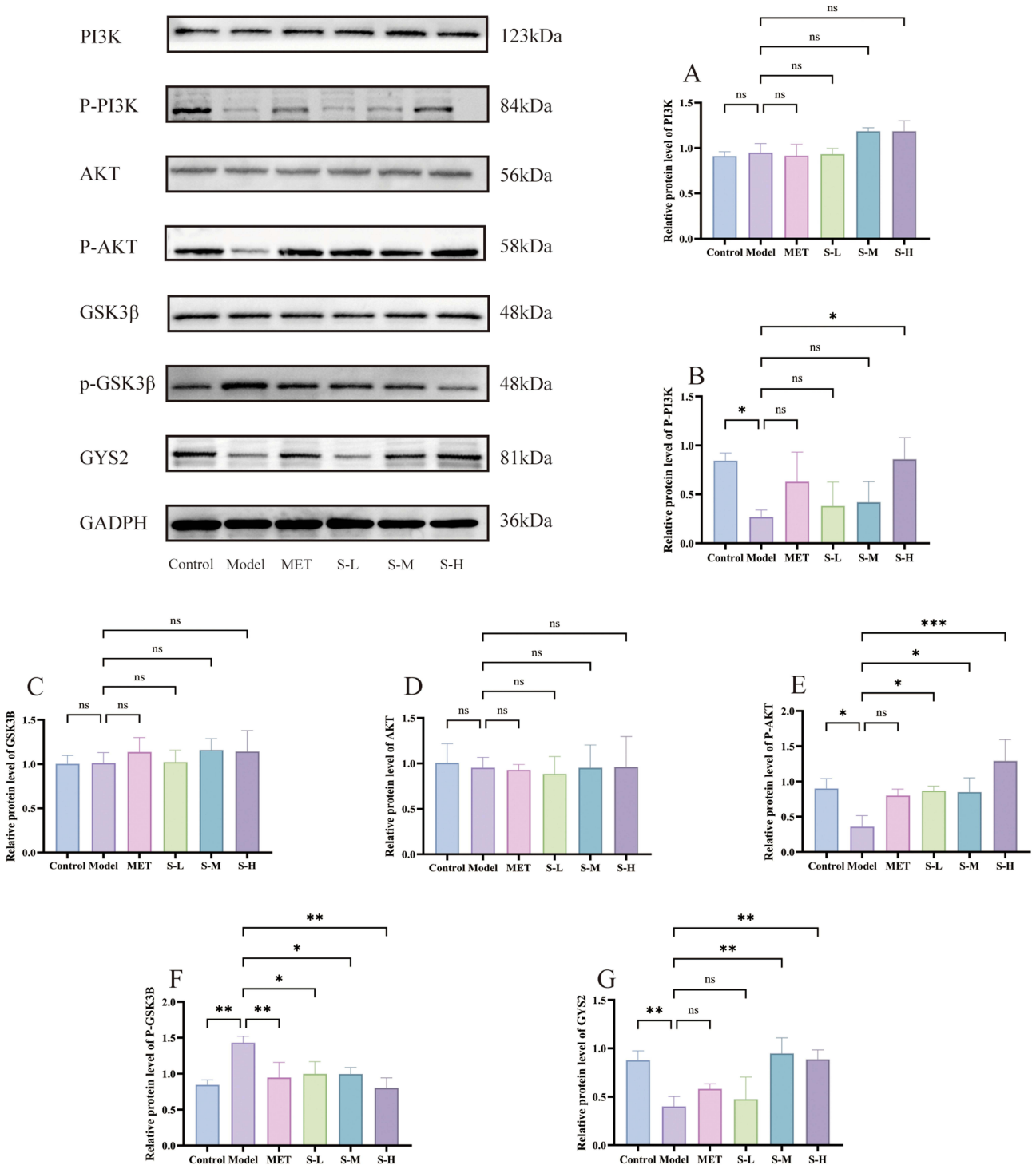

Figure 10 Western Blot results of PI3K, P-PI3K, AKT, P-AKT, GSK3B, P-GSK3B, and GYS2. (**A**) Relative protein expression of PI3K. (**B**) Relative protein expression of P-PI3K. (**C**) Relative protein expression of GSK3B. (**D**) Relative protein expression of AKT. (**E**) Relative protein expression of P-AKT. (**F**) Relative protein expression of P-GSK3B. (**G**) Relative protein expression of GYS2. *P<0.05 and **P<0.01 vs Control group; *P<0.05, **P<0.01 and ***P < 0.001 vs Model group.

significantly impact overall glucose and lipid metabolism. These conditions show up as decreased insulin sensitivity in target tissues, like liver receptors, which impairs peripheral tissues' ability to absorb glucose and causes abnormalities in the liver's glucose production. Increased insulin resistance and blood glucose levels can also contribute to other conditions, including obesity, fatty liver, polycystic ovary syndrome, and atherosclerosis.[27] SMS is a traditional herbal

https://doi.org/10.2147/DMSO.S507953

formula known for its simple yet balanced composition, which promotes qi, fluid regulation, yin nourishment, and antiperspiration effects. Reports indicate that SMS, combined with Liuwei Dihuang Decoction, can enhance blood sugar control, showing more pronounced therapeutic effects compared to conventional Western medicine.[28,29] The ingredients in SMS are believed to improve insulin sensitivity, and exert antioxidant and anti-inflammatory effects, contributing to its potential therapeutic benefits for T2DM. However, the exact mechanism of its action remains unclear.[30] Through the potential stimulation of the PI3K/AKT pathway, this study discovered that SMS reduces the pathological states of oxidative stress, inflammation, liver IR, and abnormalities of glucose and lipid metabolism in T2DM rats.

Lipid metabolism disorder is a key characteristic of T2DM. LDL-C, HDL-C, and TG are major components of body fat. Excessive TG levels can lead to fatty liver, obesity, and pancreatitis. HDL-C encourages reverse cholesterol transport from the periphery to the liver, whereas LDL-C helps transport and deposit cholesterol from the liver to peripheral tissues. IR disrupts liver tissue structure, impairs the normal functions of LDL-C and HDL-C, and reduces triglyceride clearance, leading to elevated TG levels.[31] Hypertriglyceridemia is frequently associated with adipocyte hypertrophy and hyperplasia. Enlarged adipocytes secrete TNF-α and IL-6, which promote insulin resistance. Elevated TNF-α levels can exacerbate liver IR, stimulate liver TG synthesis and accumulation, aggravate fat deposition, and enhance the expression of inflammatory factors. Additionally, TNF-α, in synergy with other endotoxins, can worsen lipid peroxidation, cause mitochondrial dysfunction in adipocytes, trigger oxidative stress, and overload fatty acid β-oxidation. This ultimately leads to further liver fat deposition and increases in serum TC, TG, and LDL-C levels.[32] In this study, SMS significantly reduced serum TC, TG, and LDL-C levels, increased HDL-C levels, and improved dyslipidemia in T2DM rats.

One important factor in the emergence of IR is low-grade inflammation. Pro-inflammatory cytokines, including TNF-α and IL-6, are secreted when inflammatory signaling pathways are activated, disrupting insulin signaling trans-activation.[33] The first and most important endogenous mediator in the inflammatory process is TNF-α.[34] T2DM can cause abnormal lipid accumulation in the liver and increased production of pro-inflammatory cytokines, such as IL-6 and TNF-α. TNF-α also promotes the secretion of additional inflammatory factors, including IL-6 and IL-17, intensifying the inflammatory cascade, leading to pathological damage, and accelerating the progression of IR.[35] Moreover, TNF-α is linked to the onset of diabetic complications and exacerbates systemic inflammation in diabetic patients.[36] In this study, SMS significantly reduced IL-6 and TNF-α levels in the rat liver, suggesting that SMS can alleviate the inflammatory response, improving pathological damage and potentially reducing diabetic complications.

Numerous antioxidant compounds have been found in studies to help stop, slow, or even treat the progression of T2DM.[37] Studies have demonstrated that modulating oxidative stress-related molecules can enhance islet cell function, promote glucose metabolism, and mitigate liver tissue damage.[38] Oxidative stress triggered by high sugar and fat intake is a major factor in the apoptosis of islet beta cells.[39] Oxidative stress can induce IR, which is closely linked to the onset and progression of T2DM.[40,41] MDA is the final product of lipid peroxidation, and its levels reflect the extent of lipid peroxidation. SOD is a key free radical scavenger; lower levels indicate reduced antioxidant capacity, while higher levels suggest stronger antioxidant defenses. After SMS administration, MDA levels decreased, and SOD activity increased in T2DM rats, suggesting that SMS can counteract oxidative stress and has a protective effect on the body in T2DM.

The PI3K/AKT/GSK3B pathway is a well-established insulin signaling pathway. Disruption of this pathway impairs the liver's ability to uptake and utilize glucose, leading to increased gluconeogenesis, reduced glycogen synthesis, enhanced glycogen release, and elevated blood glucose levels. Fujie Yan et al[42] found that MAE activation of the PI3K/AKT pathway significantly reduced high glucose/Pa-induced IR in HepG2 cells.

The PI3K/AKT pathway controls the metabolism of glucose on several levels.[43,44] Activated AKT plays a key role in insulin signaling by phosphorylating various metabolically important targets, such as GSK3B and GYS2. GYS2 is primarily expressed in the liver,[45] where its active state facilitates the conversion of blood glucose into glycogen. Pathological studies[46] indicate that GYS2 deficiency can cause glycogen storage disease type 0 (GSD-0), characterized by impaired glucose tolerance. During liver glycogen metabolism, GYS2 is inhibited by GSK3B, and GSK3B activation can inactivate GYS2.[47,48] When GSK3B is not inhibited by phosphorylation, it suppresses GYS2, preventing glycogen synthesis. This leads to reduced glycogen storage in the liver and muscles, contributing to elevated blood glucose levels. Following the administration of SMS in type 2 diabetic rats, the p85 subunit of PI3K binds to phosphorylated insulin receptor substrate (IRS) through its SH2 domain, facilitating the activation of PI3K and leading to the production of

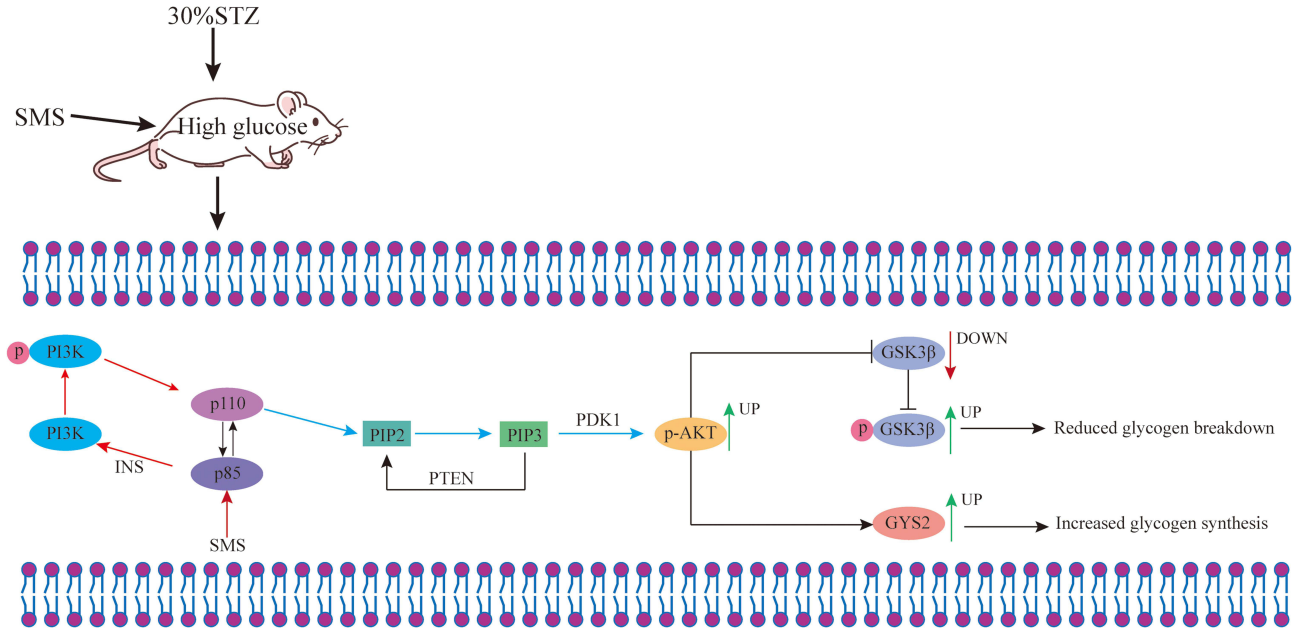

Figure 11 Molecular mechanism of SMS intervening T2DM.

phosphorylated PI3K (P-PI3K) at Tyr607. Additionally, p85 inhibits the autonomous activity of p110, preventing its overactivation. The p110 subunit of PI3K catalyzes the phosphorylation of phosphatidylinositol-4,5-diphosphate (PIP2) to generate phosphatidylinositol-3,4,5-triphosphate (PIP3), which serves as a crucial signal for the activation of downstream signaling molecules, including AKT. Upon activation, phosphorylated AKT (P-AKT) at Ser473 phosphorylates GSK3B at Ser389, thereby inhibiting its activity. In addition to reducing glycogen decomposition, the inhibition of glycogen synthase 2 (GYS2) is relieved, enhancing its function and promoting glycogen synthesis (Figure 11).[49,50]

This study investigates the mechanism of action of SMS active ingredients in treating T2DM using network pharmacology. The results indicate that seven components may affect the pharmacodynamics of T2DM by activating the PI3K/AKT, Ca2+, and cAMP signaling pathways. Among these, the PI3K/AKT pathway is strongly associated with key physiological processes, including cell proliferation, apoptosis, and autophagy. T2DM rat model was established by administering a high-sugar, high-fat diet combined with STZ intraperitoneal injection. Network pharmacological analysis suggests that SMS active components may modulate T2DM treatment by targeting the PI3K/AKT pathway. Western blot analysis revealed that following SMS administration, the expression of P-PI3K, P-AKT, GYS2, and P-GSK3B proteins significantly changed compared to the model group, supporting the hypothesis that SMS components treat T2DM by activating the PI3K/AKT pathway. In the model group, insulin receptor damage prevented PI3K activation, thereby inhibiting the generation of PIP3 and activation of AKT. This led to elevated GSK3B levels, reduced GYS2 levels, increased glycogenolysis, impaired glucose uptake, and elevated blood glucose. Following SMS treatment, insulin receptor sensitivity was enhanced. PIP3 generated by PI3K activated AKT, inhibited GSK3B phosphorylation, reduced GSK3B levels, increased GYS2 content, and enhanced glycogen synthesis and glucose uptake, leading to decreased blood glucose and contributing to T2DM treatment.

Multi-target synergism is its potential advantage. SMS demonstrates distinct advantages in regulating key physiological processes in T2DM, including glucose and lipid metabolism, oxidative stress, and inflammatory responses. However, this study has limitations such as limited sample size, single-pathway studies that may ignore other possible therapeutic mechanisms, and lack of long-term clinical validation. Therefore, the future needs to further evaluate the efficacy, safety and potential clinical applications of SMS through large-scale clinical studies and more in-depth mechanism exploration. The above has been incorporated into the final paragraph of the discussion.

https://doi.org/10.2147/DMSO.S507953

Conclusion

In this study, T2DM rat model was established using a high-fat, high-sugar diet combined with an intraperitoneal injection of STZ, followed by intragastric administration of SMS. SMS treatment improved body weight and reduced excessive water intake in T2DM rats. It decreased serum levels of TC, TG, LDL-C, MDA, TNF-α, and IL-6, while increasing SOD and HDL-C levels. It reduced insulin resistance, corrected glucose tolerance, and successfully regulated insulin and fasting blood glucose. Glycogen synthesis enhancement and PI3K/AKT pathway activation may be the underlying mechanisms.

Data Sharing Statement

The raw data supporting the conclusions of this article will be made available by the authors, without undue reservation.

Ethics Statement

This study has been approved by the Experimental Animal Welfare Ethics Review Committee of Shandong University of Traditional Chinese Medicine, approval number SDUTCM20240327003, in accordance with the relevant ethical guidelines. The study was conducted in accordance with the local legislation and institutional requirements. According to the national legislation guidelines of China, specifically Article 32, Items 1 and 2 of the Measures for Ethical Review of Life Science and Medical Research Involving Human Subjects (February 18, 2023), this study is exempt from ethical approval. The use of publicly available data, including the Database, complies with these exemption guidelines.

Acknowledgments

All claims expressed in this article are solely those of the authors and do not necessarily represent those of their affiliated organizations, or those of the publisher, the editors and the reviewers. Any product that may be evaluated in this article, or claim that may be made by its manufacturer, is not guaranteed or endorsed by the publisher.

Funding

The authors declare that financial support was received for the research, authorship, and/or publication of this article. This study is supported by the Shandong Province key research and development plan project (N0.2021CXGC010511)), Innovation Ability Improvement Project of Science and Technology smes in Shandong Province (NO.2023TSGC0271) and 2023 National traditional Chinese medicine characteristic technology inheritance talent training project (N0. T20234832005).

Disclosure

The authors declare that the research was conducted in the absence of any commercial or financial relationships that could be construed as a potential conflict of interest.

References

1. Lovic D, Piperidou A, Zografou I, et al. The growing epidemic of diabetes mellitus. *Curr Vasc Pharmacol*. 2020;18(2):104–109. doi:10.2174/1570161117666190405165911
2. Beckman JA, Creager MA, Libby P. Diabetes and atherosclerosis - Epidemiology, pathophysiology, and management. *JAMA J Am Med Assoc*. 2002;287(19):2570–2581. doi:10.1001/jama.287.19.2570
3. Jiana H, Guoliang C, Zhiwei H, et al. Research progress of Shenqi Jiangtang granules in prevention and treatment of disorders of glucose and lipid metabolism. *Chin Traditional Herbal Drugs*. 2022;53(17):5544–5552.
4. Tian L. Clinical observation on the efficacy and safety of liraglutide in type 2 diabetic patients with poor glycemic control. 2016.
5. Chen W, Wang J, Luo Y, et al. Ginsenoside Rb1 and compound K improve insulin signaling and inhibit ER stress-associated NLRP3 inflammasome activation in adipose tissue. *J Ginseng Res*. 2016;40(4):351–358. doi:10.1016/j.jgr.2015.11.002
6. Qiu Z, Dong J, Xue C, et al. Liuwei Dihuang Pills alleviate the polycystic ovary syndrome with improved insulin sensitivity through PI3K/Akt signaling pathway. *J Ethnopharmacol*. 2020;250:111965. doi:10.1016/j.jep.2019.111965
7. Kuan IHS, Savage RL, Duffull SB, et al. The association between metformin therapy and lactic acidosis. *Drug Safety*. 2019;42(12):1449–1469. doi:10.1007/s40264-019-00854-x
8. Odawara M, Kawamori R, Tajima N, et al. Long-term treatment study of global standard dose metformin in Japanese patients with type 2 diabetes mellitus. *Diabetol Int*. 2017;8(3):286–295. doi:10.1007/s13340-017-0309-z

9. Lalau J-D, Kajbaf F, Arnouts P, et al. Mortality and metformin use in patients with advanced chronic kidney disease. *Lancet Diabetes Endocrinol*. 2015;3(9):680–681. doi:10.1016/s2213-8587(15)00285-5
10. Yin F. Causes and clinical analysis of hypoglycemia in elderly diabetic patients treated with insulin pump. *China Med Device Information*. 2020;26 (12):153–154. doi:10.15971/j.cnki.cmdi.2020.12.075
11. Luo W, Wang X. Study on quenching thirst in Huangdi Neijing. *J Shandong University Chin Med*. 2018;42(04):292–295. doi:10.16294/j.cnki.1007-659x.2018.04.005
12. Wu T. The main pathological sites and pathogenesis of diabetes in ancient literature. *Chinese Med Guide*. 2008;6(23):301–303.
13. Yan H, Yin C, Zhao Y, et al. Clinical observation of Huangqin Talshi Decoction treating 60 cases of spleen type 2 diabetes trapped by dampness-heat. *Chin Nat Folk Med*. 2019;28(07):100–102.
14. Wu B, Sui M, Zhu Y, et al. Sanhuang Decoction treated 43 cases of phlegm-dampness-heat-junction type 2 diabetes mellitus. *Henan Trad Chin Med*. 2019;39(06):839–842. doi:10.16367/j.issn.1003-5028.2019.06.0208
15. Hao X. Wuling Powder was used to treat 49 cases of diabetic nephropathy. *Henan Trad Chin Med*. 2017;37(10):1715–1717. doi:10.16367/j.issn.1003-5028.2017.10.0596
16. Yoon JJ, Lee YJ, Lee SM, et al. Oryeongsan suppressed high glucose-induced mesangial fibrosis. *BMC Complementary Alternative Med*. 2015;15 (1). doi:10.1186/s12906-015-0542-6
17. Cao Z, Pan J, Li N, et al. Research progress of modern pharmacological action and mechanism of Shengmai Powder. *J Chin Experimental Formulae*. 2019;25(22):212–218. doi:10.13422/j.cnki.syfjx.20192208
18. Cheng Y, Jing R, Tan J, et al. Research progress of modern pharmacology and mechanism of action of Shengmai Powder. *J Liaoning University Chin Med*. 2016;18(05):253–256. doi:10.13194/j.issn.1673-842x.2016.05.084
19. Li H, Jia N. Research progress of Shengmai Powder. *J Liaoning University Chin Med*. 2020;22(10):190–193. doi:10.13194/j.issn.1673-842x.2020.10.045
20. Ru JL, Li P, Wang JN, et al. TCMSP: a database of systems pharmacology for drug discovery from herbal medicines. *J Cheminf*. 2014;6(1). doi:10.1186/1758-2946-6-13
21. Daina A, Michielin O, Zoete V. Swiss Target Prediction: updated data and new features for efficient prediction of protein targets of small molecules. *Nucleic Acids Res*. 2019;47(W1):W357–W364. doi:10.1093/nar/gkz382
22. Piñero J, Ramírez-Anguita JM, Saüch-Pitarch J, et al. The DisGeNET knowledge platform for disease genomics: 2019 update. *Nucleic Acids Res*. 2020;48(D1):D845–D855. doi:10.1093/nar/gkz1021
23. Stelzer G, Plaschkes I, Oz-Levi D, et al. VarElect: the phenotype-based variation prioritizer of the genecards suite. *Bmc Genomics*. 2016;17(S2). doi:10.1186/s12864-016-2722-2
24. Sherman BT, Hao M, Qiu J, et al. DAVID: a web server for functional enrichment analysis and functional annotation of gene lists (2021 update). *Nucleic Acids Res*. 2022;50(W1):W216–W221. doi:10.1093/nar/gkac194
25. Niu JM, Xu GY, Jiang S, et al. In Vitro Antioxidant activities and anti-diabetic effect of a polysaccharide from Schisandra sphenanthera in rats with type 2 diabetes. *Int J Biol Macromol*. 2017;94:154–160. doi:10.1016/j.ijbiomac.2016.10.015
26. Zimmet P, Alberti K, Shaw J. Global and societal implications of the diabetes epidemic. *Nature*. 2001;414(6865):782–787. doi:10.1038/414782a
27. Saltiel AR. Insulin signaling in health and disease. *J Clin Investig*. 2021;131(1). doi:10.1172/jci142241
28. Huang J. Observation on the effect of Shengmai Powder combined with Liuwei Dihuang Decoction in the treatment of diabetes mellitus and blood sugar level. *J Rare Dis*. 2023;30(10):91–92+99.
29. Luo C. Evaluation of curative effect and effective rate of Shengmai Powder combined with Liuwei Dihuang Decoction in the treatment of diabetes. *New World Diabetes*. 2021;24(20):108–111. doi:10.16658/j.cnki.1672-4062.2021.20.108
30. Li SL, Qian Y, Xie R, et al. Exploring the protective effect of ShengMai-Yin and Ganmaidazao decoction combination against type 2 diabetes mellitus with nonalcoholic fatty liver disease by network pharmacology and validation in KKAy mice. *J Ethnopharmacol*. 2019;242:112029. doi:10.1016/j.jep.2019.112029
31. Zhu H, Guan H, Yan H, et al. Research progress on prevention and treatment of liver insulin resistance in type 2 diabetes mellitus by regulating PI3K/Akt signaling pathway with traditional Chinese medicine. *Jilin Trad Chin Med*. 2023;43(11):1356–1360. doi:10.13463/j.cnki.jlzyy.2023.11.025
32. Wang X, Li W, Zhang H, et al. Effects of schisandra and glycyrrhiza combination on blood lipid regulation and synthesis pathway of triglycerides. *Chinese Pharmacol Bulletin*. 2021;37(01):136–142.
33. Zhang H, Gao X, Li K, et al. Sandalwood seed oil ameliorates hepatic insulin resistance by regulating the JNK/NF-κB inflammatory and PI3K/AKT insulin signaling pathways. *Food Funct*. 2021;12(5):2312–2322. doi:10.1039/d0fo03051a
34. Brånén L, Hovgaard L, Nitulescu M, et al. Inhibition of tumor necrosis factor-α reduces atherosclerosis in apolipoprotein E knockout mice. *Arterioscler Thrombosis Vasc Biol*. 2004;24(11):2137–2142. doi:10.1161/01.ATV.0000143933.20616.1b
35. Hou L, Liu Y, Shu S. Relationship between the relative expression levels of miR-18a and miR-125b in peripheral blood mononuclear cells and glucose and lipid metabolism, inflammatory factors and insulin resistance in patients with type 2 diabetes mellitus. *Int J Lab Med*. 2021;42 (18):2190–2194+2199.
36. Lan F, Mou Y, Shou L, et al. Correlation between levels of hypersensitive C-reactive protein, IL-6, TNF-α and secondary infection in type 2 diabetic ketoacidosis. *Lab Med Clin*. 2019;16(22):3315–3316+3320.
37. Hao J, Niu H, Liu Y, et al. The role of oxidative stress in diabetic nephropathy and the progress of antioxidant therapy. *J Neuropharmacol*. 2020;10 (02):33–38.
38. Sun B, Jia Y, Yang S, et al. Sodium butyrate protects against high-fat diet-induced oxidative stress in rat liver by promoting expression of nuclear factor E2-related factor 2. *Br J Nutr*. 2019;122(4):400–410. doi:10.1017/S0007114519001399
39. Minn AH, Hafele C, Shalev A. Thioredoxin-interacting protein is stimulated by glucose through a carbohydrate response element and induces β-cell apoptosis. *Endocrinology*. 2005;146(5):2397–2405. doi:10.1210/en.2004-1378
40. Cai L, Li W, Wang G, et al. Hyperglycemia-induced apoptosis in mouse myocardium: mitochondrial cytochrome C-mediated caspase-3 activation pathway. *Diabetes*. 2002;51(6):1938–1948. doi:10.2337/diabetes.51.6.1938
41. Wei W, Liu QJ, Tan Y, et al. OXIDATIVE STRESS, DIABETES, AND DIABETIC COMPLICATIONS. *Hemoglobin*. 2009;33(5):370–377. doi:10.3109/03630260903212175

42. Yan F, Dai G, Zheng X. Mulberry anthocyanin extract ameliorates insulin resistance by regulating PI3K/AKT pathway in HepG2 cells and db/db mice. *J Nutr Biochem*. 2016;36:68–80. doi:10.1016/j.jnutbio.2016.07.004
43. Gao J, Li J, An Y, et al. Increasing effect of Tangzhiqing formula on IRS-1-dependent PI3K/AKT signaling in muscle. *BMC Complement Altern Med*. 2014;14(1):198. doi:10.1186/1472-6882-14-198
44. Gao Y, Zhang M, Wu T, et al. Effects of d -Pinitol on insulin resistance through the PI3K/Akt signaling pathway in Type 2 diabetes mellitus rats. *J Agric Food Chem*. 2015;63(26):6019–6026. doi:10.1021/acs.jafc.5b01238
45. Nessa A, Kumaran A, Kirk R, et al. Mutational analysis of the GYS2 gene in patients diagnosed with ketotic hypoglycaemia. *J Pediatr Endocrinol Metab*. 2012;25(9–10):963–967. doi:10.1515/jpem-2012-0165
46. Weinstein DA, Correia CE, Saunders AC, et al. Hepatic glycogen synthase deficiency: an infrequently recognized cause of ketotic hypoglycemia. *Mol Gene Metabol*. 2006;87(4):284–288. doi:10.1016/j.ymgme.2005.10.006
47. Kamenets EA, Gusarova EA, Milovanova NV, et al. Hepatic glycogen synthase (GYS2) deficiency: seven novel patients and seven novel variants. *JIMD Rep*. 2020;53(1):39–44. doi:10.1002/jmd2.12082
48. Wang LJ, Zuo B, Xu DQ, et al. Alternative splicing of the porcine glycogen synthase kinase 3β (GSK-3β) gene with differential expression patterns and regulatory functions. *PLoS One*. 2012;7(7). doi:10.1371/journal.pone.0040250
49. Doi R, Oishi K, Ishida N. CLOCK regulates circadian rhythms of hepatic glycogen synthesis through transcriptional activation of Gys2. *J Biol Chem*. 2010;285(29):22114–22121. doi:10.1074/jbc.M110.110361
50. Cross DA, watt PW, Shaw M, et al. Insulin activates protein kinase B, inhibits glycogen synthase kinase-3 and activates glycogen synthase by rapamycin-insensitive pathways in skeletal muscle and adipose tissue. *FEBS Lett*. 1997;406(1–2):211–215. doi:10.1016/s0014-5793(97)00240-8